2011-01-0690

Fuzzy Knock Control of Diesel-Dual-Fuel Engine

Withit Chatlatanagulchai and Kittipong Yaovaja
Faculty of Engineering, Kasetsart University

Shinapat Rhienprayoon and Krisada Wannatong
PTT Research and Technology Institute, PTT Public Company Limited

ABSTRACT

Knock behavior in diesel-dual-fuel (DDF) engine is more complex, more severe, and different than those of traditional engines. We investigate a type of diesel-dual-fuel engines, where CNG is multipoint-injected at the intake ports as main fuel and diesel is directly injected in smaller amount, mainly for ignition purpose, resulting in lower fuel cost. Because of the mixed behaviors between the spark ignited and compression ignited engines, a more sophisticated control system is needed to properly control knock in the DDF engine. In this paper, a novel control system based on fuzzy logic is presented to regulate knock intensity at an appropriate level. The control system comprises a fuzzy controller and a fuzzy decision maker. The fuzzy controller controls several pertaining actuators using rule-base from human experience, while the fuzzy decision maker adapts the magnitude of each actuator action to various operating points. From an engine test bed data, the in-cylinder pressure was compared to the knock sensor signal to select a frequency range to consider. An existing frequency-domain knock intensity detection algorithm was applied to detect the knock intensity in real time. Then the control system was designed to adjust several parameters, including CNG and diesel amount, diesel injection timing, rail pressure, and throttle and EGR set points, for the engine to operate near the knock intensity limit. A switching algorithm was added to prioritize the actuators. The control system was trialed with an engine test bed, programmed to run an NEDC test. The proposed algorithm has shown excellent result in regulating knock. The DDF engine was able to operate closer to the optimal points, resulting in more CNG use at most operating points.

INTRODUCTION

The use of methane such as natural gas and bio-methane as alternative fuel can reduce emissions as well as increase security of supply. Methane has low hydrogen-to-carbon ratio resulting in low CO_2 emissions per energy content. Because of the short carbon chains in methane, methane gas also generally produces low particulate emissions. Methane gas is also abundant in the gulf of Thailand.

The majority of heavy-duty trucks use diesel engine. Retrofitting diesel engines to run on methane has two options, with and without electrical spark plugs. With spark plugs, combustion system is changed from the diesel-cycle to the Otto-cycle by changing pistons. Without spark plugs, the so-called diesel-dual-fuel (DDF) engine, both diesel and methane gas are used simultaneously, where diesel is directly injected mainly for ignition and methane is used for energy supply. The small diesel injection ignites the methane like a "liquid" spark plug, introducing far more energy than the electrical spark plug, which increases the lean burn capability compared to the with-spark-plug case.

In the DDF engines, methane is either injected at the intake ports creating "premixed" air/methane mixture or directly injected into the combustion chamber. Compared to the direct injected system, the premixed system has higher level of unburned methane and has knock limited gas replacement over the full operating range of the engine, but is less expensive, simpler to install, and can operate in diesel-only mode. The advantages of the premixed system seem to outweigh its disadvantages, making it the most common DDF system.

In the premixed DDF engines, methane can be injected at a single point or at multiple points. In single-point injection, methane for all cylinders is injected at one location, normally in front of the throttle. In multi-point injection, there is at least one gas injector for every cylinder, located at its intake port. Compared to the single-point injection, the multi-point injection has worse homogenous mixture between the gas and air and more cylinder-to-cylinder air-to-fuel (A/F) ratio variation, but has better transient A/F ratio control and better fuel cut capability.

Methane resists knock, reflecting in very high octane number. However, the natural gas also contains heavier hydrocarbons such as ethane and propane, which deteriorates the high knock resistance of the pure methane.

We focus on retrofitting heavy-duty truck diesel engines as DDF engines. Our engine is premixed system with multi-point injection. Compressed natural gas (CNG) is used as methane gas. Our DDF engines experience heavy knock when using high diesel replacement at high loads, transient knocks during sudden load and speed changes, and hard combustion, caused by high in-cylinder pressure gradient. It is evident that our knock problem is complex, involving several actuators, and is in need of a sophisticated knock control algorithm.

Existing knock control methods can be separated into event-based and intensity-based methods. In event-based methods, when knock intensity is above a threshold, a knock event is said to occur, and a fixed amount of corrective action is applied. For example, in SI engines, when a knock event occurs, the ignition timing is retarded by a fixed amount, followed by small ignition timing advances until a new knock event is detected, then the whole process starts again. The disadvantages of this method are a right threshold that does not create missed detection or false detection is difficult to find, the fixed corrective action usually results in non-optimum engine operations, the counter corrective actions can promote increased knock occurrence rate, and only one corrective action applies at a time. Adaptive knock control, presented in [1], reduced the knock occurrence rate from counter corrective actions, but non-optimum engine operations were still present.

In intensity-based methods, knock intensity is regulated at appropriate set-points. As a result, the engines can be operated near optimal performance without knock. Examples of the intensity-based knock control are as follows. Ref. [2] regulated borderline knock for SI engines using closed-loop stochastic limit controls with in-cylinder ionizaton signals. Ref. [3] used hybrid modeling and model predictive control to control air path of a gasoline engine to avoid knock. Ref. [4] applied fuzzy control to regulate knock of an SI engine. Ref. [5] patented a knock control using fuzzy logic. The success of the intensity-based methods depends heavily on the accuracy of knock identification to determine the knock intensity.

Knock identification methods can be divided into time-domain methods and frequency-domain methods. In practice, signals from knock sensors attached to the engine crank case are amplified, band-passed, rectified, windowed, then integrated to give knock intensity. Several more-advanced knock identification methods have also existed in the literature. Ref. [6] measured knock intensity using a parametric model-based filter. Ref. [7] - [10] used wavelet transform to detect knock. Ref. [11] applied short-term-Fourier-transform to identify engine knock from various sources of engine-block vibration. Ref. [12] reconstructed the in-cylinder pressure signal from vibration sensors using the Volterra model. Ref. [13] presented a frequency-domain method called recursive trigonometric interpolation to calculate knock intensity.

Other noteworthy works pertaining to knock control are as follows. Ref. [14] - [16] studied knock behavior of a one-cylinder engine test bed modified as a DDF engine. Ref. [17] - [20] used knock sensor signal in real-time computation of estimated combustion parameters used in control of combustion timing of Homogeneous Charge Compression Ignition (HCCI) engines. Ref. [21] presented knock prediction and preventive of stationary SI gas engines. The knock prediction is obtained from engine operating conditions and fuel gas methane number, and the knock preventive acts on the engine load before knock happens. Ref. [22] used methane-air mixture chemical kinetics to predict knock in dual-fuel engines.

We used two fuzzy systems, one is called fuzzy controller, the other is called fuzzy decision maker. The fuzzy controller received knock regulation error and its integral as inputs. A fuzzy rule-base was constructed from human experience on how to actuate several actuators in order to reduce knock regulation error. Six parameters were found to affect knock and were changed by the fuzzy controller. By controlling output gains of the fuzzy controller, the fuzzy decision maker controlled how much of these six parameters should be changed at a specific operating point. A switching algorithm was designed as a simple logic to select the order of which the six parameters are to be changed. We used the online knock identification method proposed in [13] to determine the knock intensity.

A 2KD-FTV Toyota diesel engine was modified as a DDF engine and was installed in a test cell with an engine dynamometer. The engine dynamometer was controlled by AVL PUMA, and the engine controller was National Instruments' PXI system. The new European driving cycle (NEDC) was programmed in the engine dynamometer.

We performed three cases of experiments: without control, with fuzzy controller only, and with both fuzzy controller and fuzzy decision maker. The latter case outperformed the first two cases in terms of knock regulation performance. The engine was operated smoother and closer to the optimal point. As a result, more natural gas can be used at most operating points.

The proposed knock control system has following advantages.

- Human experience can be applied directly on how to regulate knock at desired threshold
- Multiple actuators are controlled simultaneously, not just a single actuator e.g. ignition timing
- Amount of change in the parameters that affect knock is controlled by the fuzzy decision maker
- Priority of each actuator can be controlled from the switching algorithm

The paper presents topics in the following order.

- DDF engine set-up
- Knock identification
- Details of control system design
- Experimental results
- Conclusions
- References, contact information, and acknowledgments.

DDF ENGINE SET-UP

Figure 1 depicts schematic of our DDF engine. The DDF engine was modified from a 2KD-FTV Toyota diesel engine, whose specifications are given in Table 1. CNG is injected at the intake ports as in premixed case. There is one gas injector for every intake port as in multi-point injection. The EGR valve receives exhausted gas from

the manifold close to cylinder #4. There is no intercooler but one plenum. There is also one mechanical waste gate, which cannot be actuated online.

The DDF engine was installed in a test cell with an engine dynamometer. The test cell management system is AVL PUMA, and data acquisition and control hardware is National Instruments.

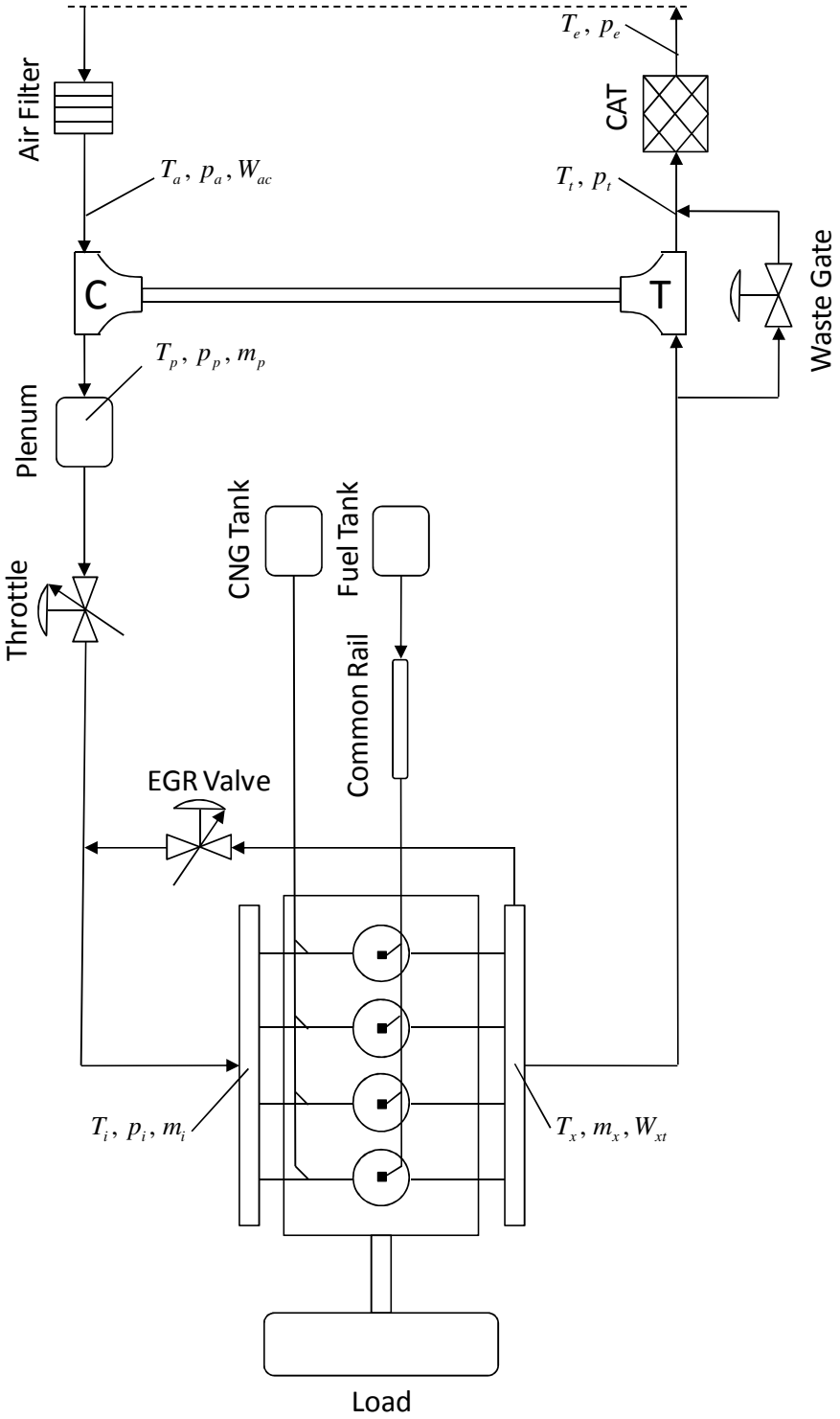

Figure 1: Overall schematic of our DDF engine.

Table 1: Engine Specifications

Model:	Toyota 2KD-FTV, Diesel Engine
Number of cylinders:	4 (Inline)
Number of valves:	16 (DOHC)
Manifold:	Cross-flow with turbocharger
Fuel system:	Commonrail direct injection
Displacement:	2,494 cc
Bore:	92.0 mm
Stroke:	93.8 mm
Connecting rod:	158.5 mm
Compression ratio:	18.5:1
Max power:	75 kW at 3,600 rpm
Max torque:	260 Nm at 1,600 - 2,400 rpm
Valve timings: IVO IVC EVO EVC	 718 deg CA 211 deg CA 510 deg CA 0 deg CA
Firing order:	1-3-4-2

Parameters in Figure 1 describe measurable quantities from the engine test bed. T, p, W, m are for temperature, pressure, mass flow rate, and mass, respectively. Subscripts a, c, p, i, x, t, e are for ambient, compressor, plenum, intake manifold, exhaust manifold, turbine, and exhaust pipe, respectively. Throttle and EGR valves are two actuators to control MAF and MAP, which are denoted by W_{ac} and p_i in Figure 1.

KNOCK IDENTIFICATION

We applied the recursive trigonometric interpolation method in [13] to calculate the frequency contents of knock signal, obtained from a knock sensor, installed on the engine crank case between cylinder#2 and #3.

Let s_k be the knock signal measured at time $t_k = k\Delta$. The signal can be approximated by the trigonometric polynomial as follows:

$$\hat{s}_k = \varphi_k^T \theta_k,$$
$$\theta_k^T = \left[a_{0k}, a_{q1k}, b_{q1k}, a_{q2k}, b_{q2k}, ..., a_{qmk}, b_{qmk} \right],$$
$$\varphi_k^T = \left[1, \cos\left(q_1 t_k\right), \sin\left(q_1 t_k\right), ..., \cos\left(q_m t_k\right), \sin\left(q_m t_k\right) \right],$$

where $\hat{s}_k$ is an approximate of s_k, θ_k is a vector of unknown coefficients, φ_k is a known vector containing basis terms, and q_i are frequencies in rad/s. This technique can be thought of as constructing a Fourier series to approximate a non-periodic, but finite function. q_i are frequencies of interest. The corresponding coefficient magnitude

$$A_{qik} = \sqrt{a_{qik}^2 + b_{qik}^2}$$

determines the q_i frequency content in the signal and can be computed using standard recursive least squares method, for example, in [23].

In our case, an in-cylinder pressure sensor was put in cylinder#2 and recorded the pressure during knock and non-knock events. From fast Fourier transform (FFT) of the pressure signal, we identified the knock frequency to be around 60,000 to 70,000 rad/s. Therefore, using the knock sensor signal, we set $q_1 = 6\times10^4\ rad/s$, $q_2 = 6.2\times10^4\ rad/s$, $q_3 = 6.4\times10^4\ rad/s$, $q_4 = 6.6\times10^4\ rad/s$, $q_5 = 6.8\times10^4\ rad/s$. The magnitude A_{qik} was found from recursive least squares method, and its values at an instant are shown in Figure 2. The blue line is a result of using knock sensor signal recorded during a knock event. The red line is a result of non-knock event. It can be seen that the frequency content during a knock event is 3-4 times in magnitude higher than during a non-knock event.

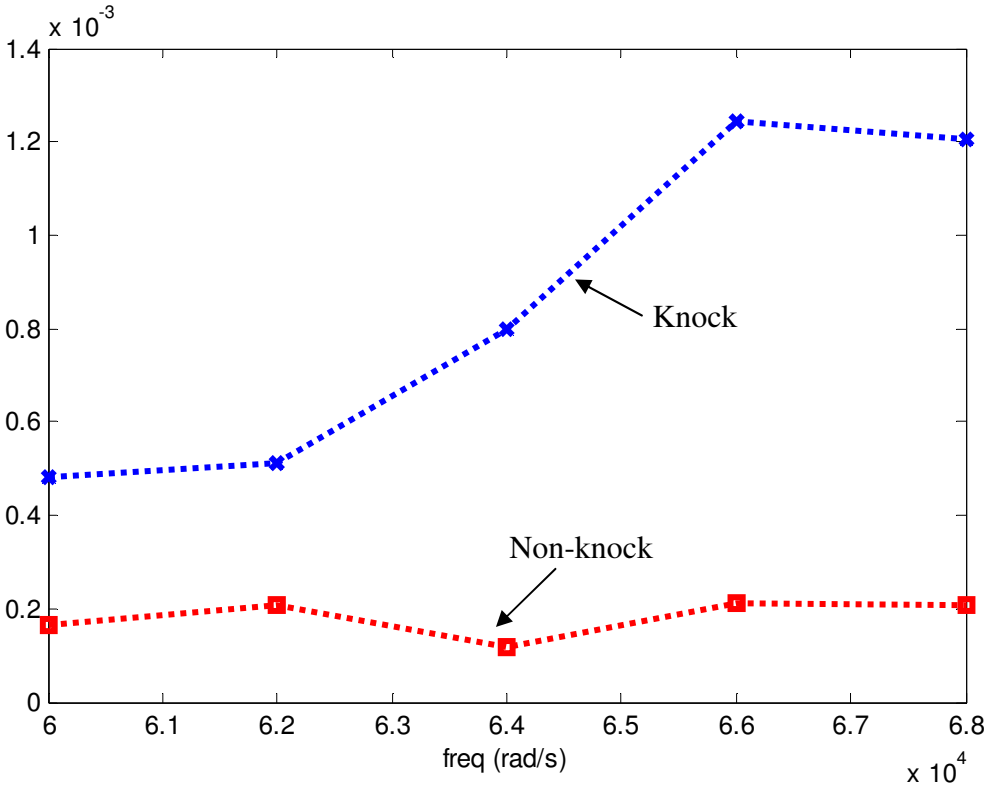

Figure 2: Comparison of the magnitude A_{qik} between knock (blue) and non-knock (red).

The root-mean-square value of A_{qik} is used as our knock intensity.

DETAILS OF CONTROL SYSTEM DESIGN

Our DDF engine experiences the following knock and knock-related incidents.

- Heavy knock when using high diesel replacement at high loads.
  This is because, in premixed system, the air/methane mixture burns with flame propagation (SI-like combustion), which is prone to knock with hot combustion chamber.
- Transient knock during sudden load decrease
  At low load, the diesel injection is forced to retard while the combustion chamber temperature is still high from high load. This knock behaves like a diesel engine knock.
- Transient knock during heavy acceleration
  During heavy acceleration, the diesel replacement is decreased, which means more diesel is used.
- Transient knock during heavy deceleration
  During heavy deceleration, the mixture has more time to auto-ignite, while the combustion chamber is still hot from running at high speed.
- Hard combustion (as characterized by high in-cylinder pressure gradient), which creates noise especially during transient.
  This incident is less severe than engine knock. However, it creates high level of audible noise, which must be decrease.

From test-cell experiments, we identified six parameters that affect knock. They are listed in Table 2 along with their suggested tuning directions to reduce knock. Some facts, which should be noted in order to understand our rationale behind the strategies in Table 2, are given as follows.

- In some operating points, we used two diesel pulses with the first pulse as main and the second pulse as post injections. The fraction of the first pulse quantity over the total diesel quantity is called "fuel split".
- SI-like combustion occurs before diesel-like combustion in the crank-angle domain.
- CNG generally resists knock better than diesel.
- In our DDF engine, we chose to actuate both throttle and Exhaust gas recirculation (EGR) valve. Throttle opening in general is proportional to the amount of fresh air entering the engine. However, EGR valve opening is inversely proportional.

Table 2: Parameters that affect knock.

Parameter	To reduce knock
Replacement ratio (a fraction of CNG over diesel)	Increase replacement ratio (use more CNG)
Diesel 1st pulse timing	Advance to avoid diesel-like knock
Fuel split (a fraction of diesel first pulse quantity over total diesel quantity)	Decrease to reduce diesel first pulse to avoid SI-like knock
Rail pressure	Decrease to reduce injection pressure
Throttle opening	Increase to obtain more air
EGR valve opening	Decrease to obtain more air

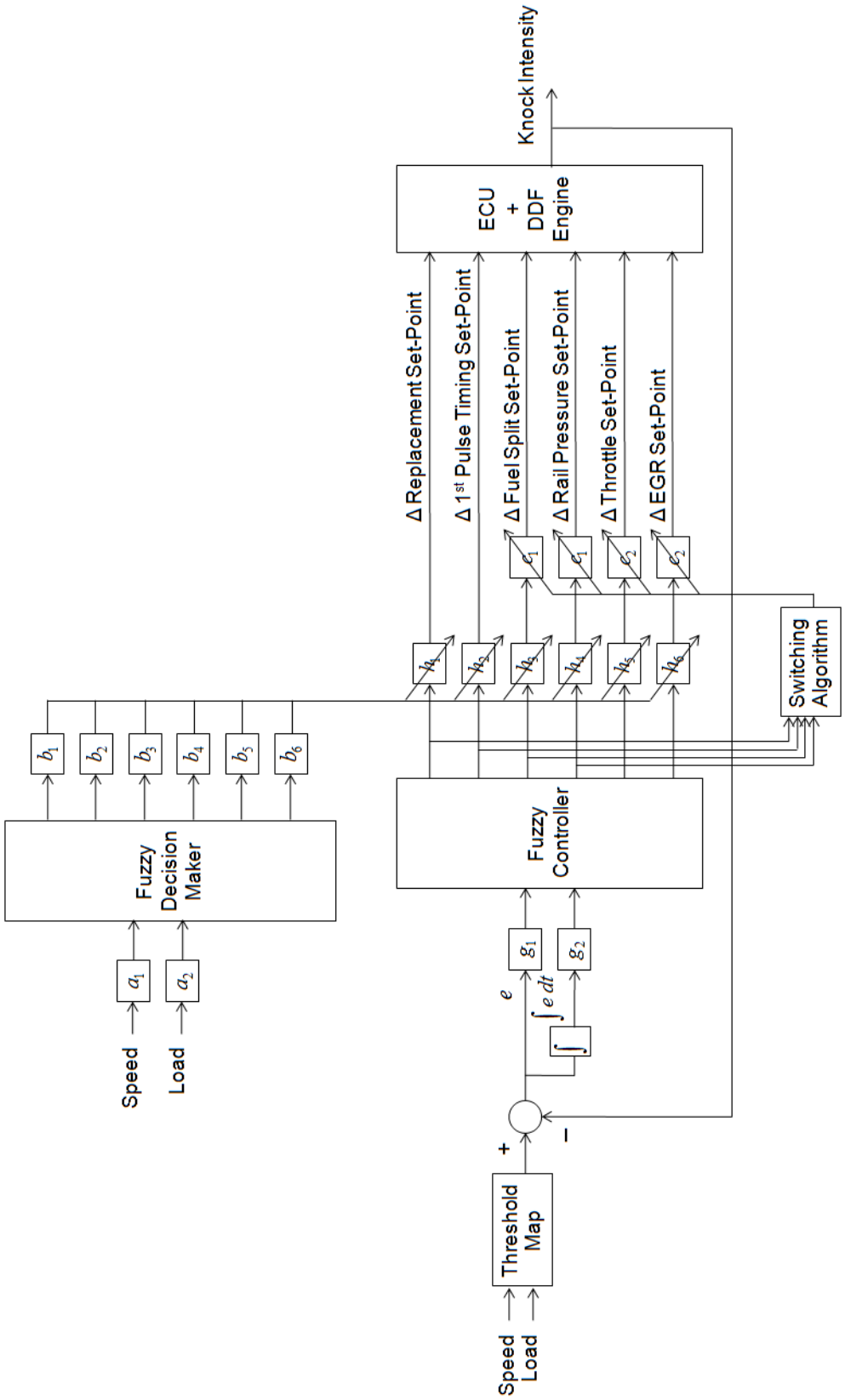

Figure 3: Knock control system consisting of a fuzzy controller, a fuzzy decision maker, and a switching algorithm.

Figure 3 shows our knock control system. There are four important parts: threshold map, fuzzy controller, fuzzy decision maker, and switching algorithm. Details of them are explained as follows.

Threshold map

Appropriate knock threshold values were determined experimentally as a function of engine speed and load. Indicated mean effective pressure (IMEP) is used as load in all our presentations.

Fuzzy controller

Knock intensity is computed on-line and is fed back to find regulating error $e(t)$ and its integral $\int e\,dt$, which are two inputs to the fuzzy controller. The input gains g_1 and g_2 are two scaling gains, which convert the inputs to a number within -1 to 1 range.

The fuzzy controller is normalized, that is, all universes of discourse are from -1 to 1. The input membership functions are given in Figure 4(a) and (b). The output membership functions are given in Figure 4(c). The premise conjunction is "minimum". The defuzzification method is center of gravity (COG).

The output gain h_1 belongs to the Δ replacement set-point. The output gain h_2 belongs to the Δ 1st pulse timing set-point. The output gain h_3 belongs to the Δ fuel split set-point. The output gain h_4 belongs to the Δ rail pressure set-point. The output gain h_5 belongs to the Δ throttle opening set-point. The output gain h_6 belongs to the Δ EGR valve opening set-point. All Δ's are added to the nominal set-points from their corresponding maps, which were obtained during steady-state calibrations. All output gains are adapted based on the outputs of the fuzzy decision maker.

Figure 6(a), Figure 7(a), Figure 8(a), and Figure 9(a) contain the rule-bases of the fuzzy systems for the Δ replacement set-point, the Δ 1st pulse timing set-point, the Δ fuel split set-point, and the Δ rail pressure set-point, respectively. Note that we use linguistic numeric values "-2" to mean "neglarge", "-1" to mean "negsmall", "0" to mean "zero", "1" to mean "possmall", "2" to mean "poslarge". Figure 6(b) to Figure 9(b) show their corresponding control surfaces. Note that the rule-bases in all cases are symmetrical, and we leave the Δ throttle set-point and the Δ EGR set-point out for now, as will be explained later in the experimental section.

Fuzzy decision maker

Engine speed and load enter the fuzzy decision maker with input scaling gains a_1 and a_2, which scale the inputs to within 0 to 1 range.

The fuzzy system is normalized such that all universes of discourse are from 0 to 1. The input membership functions are given in Figure 5(a) and (b). The output membership functions are given in Figure 5(c). The premise conjunction is "minimum". The defuzzification method is center of gravity (COG).

The output gains b_1 to b_6 adjust the outputs which are the values of the gains h_1 to h_6, respectively. Note that the b_i gains can be viewed as upper bounds of the gains h_1 to h_6.

Figure 6(c) to Figure 9(c) contain the rule-bases of the fuzzy systems for the gains h_1 to h_4, respectively. Figure 6(d) to Figure 9(d) show their corresponding control surfaces.

From Figure 6(d), it can be seen that we reduced the Δ replacement set-point gain during high load. This is from our experience that too much CNG amount can cause SI-like knock from hot combustion chamber. From Figure 7(d), we chose to adjust the Δ1st pulse timing set-point gain more toward increasing load because larger amount of diesel is used during high load tolerating more timing adjustment. From Figure 8(d), we found that during high load we should decrease the adjustment of the first pulse amount since this can affect engine performance. From Figure 9(d), we can increase the adjustment of the rail pressure with increasing load due to larger amount of diesel is used at high load.

Switching algorithm

From experiments with the test bed, we found that each parameter has different influence level on knock intensity. Δ replacement set-point and Δ 1st pulse timing set-point usually have the most effect, followed by Δ fuel split set-point and Δ rail pressure set-point. Δ throttle set-point and Δ EGR set-point have the least effect. Adjusting the throttle and the EGR valve also affects air path directly, which has detrimental effects of higher emissions. Due to this reason, we decided not to adjust them in our experiments.

We can do this by using a simple switching algorithm with two gains c_1 and c_2. We let the replacement set-point and the 1st pulse timing set-point to first adjust until they reach their maximum limit, then c_1 is changed from zero to one to allow the fuel split set-point and the rail pressure set-point to adjust until they reach their maximum limit, then c_2 is changed from zero to one to allow the throttle and EGR set-point to adjust. In case we decide not to adjust the throttle and the EGR valve, we can set c_2 to zero at all time.

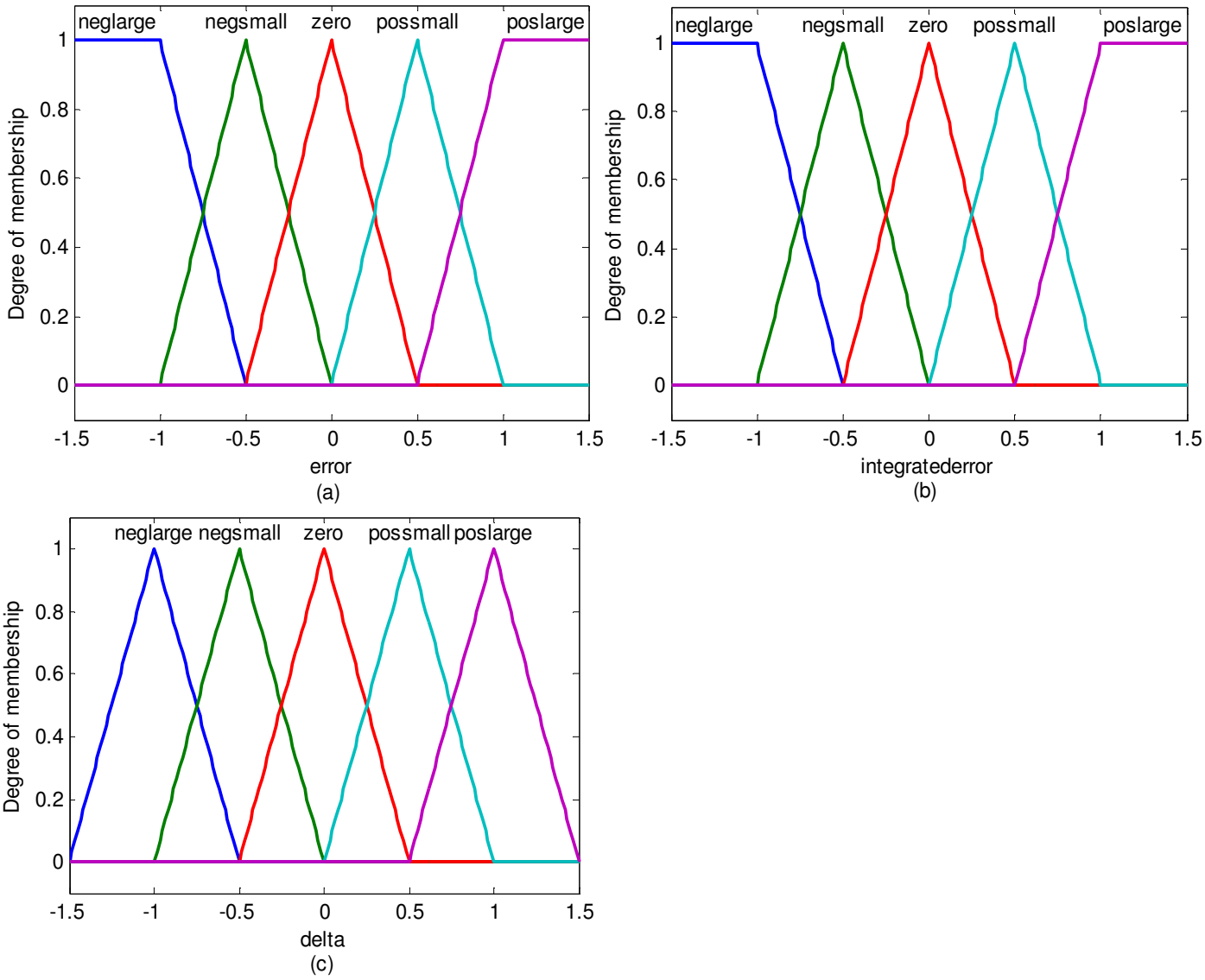

Figure 4: Fuzzy controller membership functions. (a) Input membership functions for error $e(t)$. (b) Input membership functions for integral of error $\int e\,dt$. (c) Output membership functions for actuator deviation Δ.

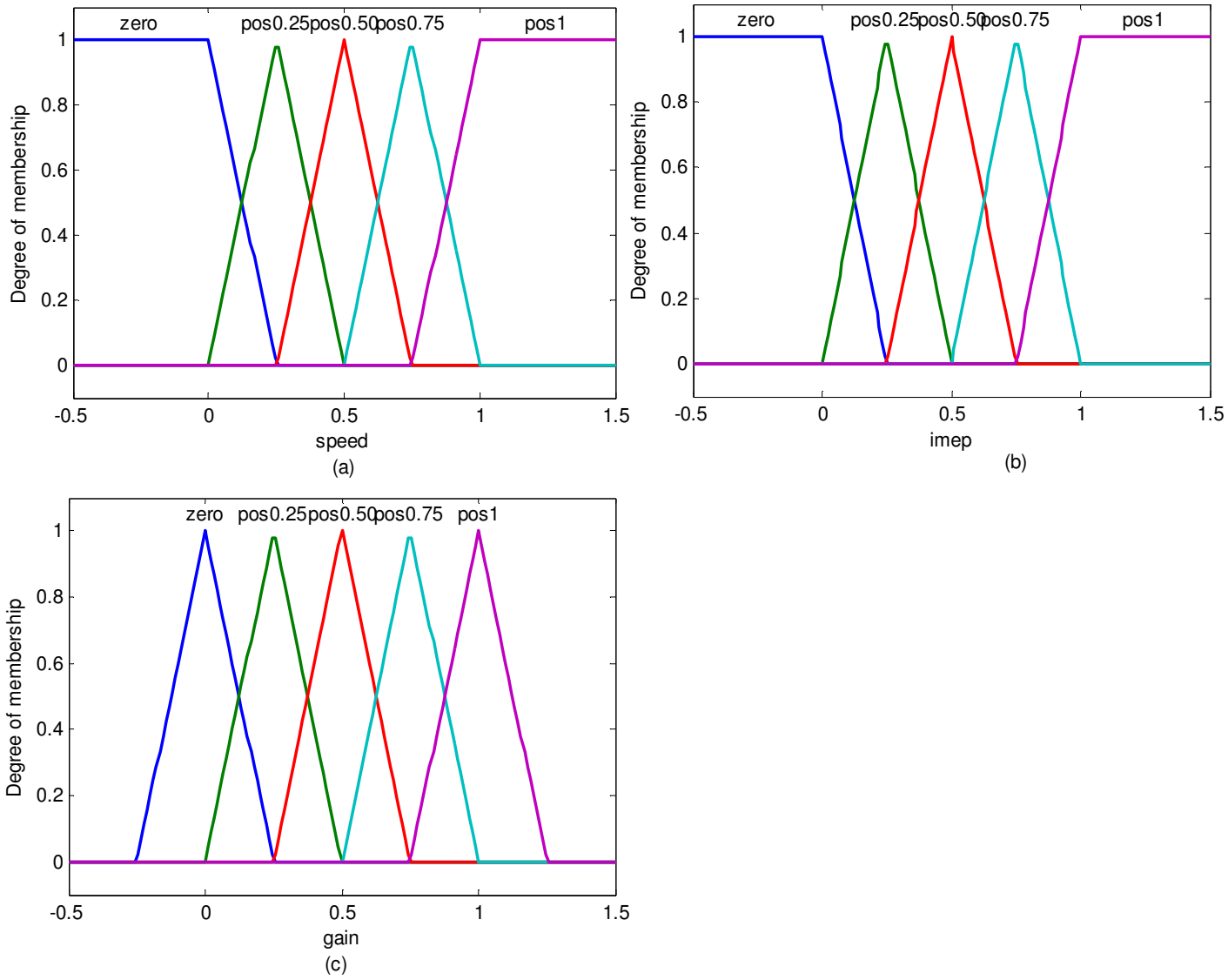

Figure 5: Fuzzy decision maker membership functions. (a) Input membership functions for engine speed. (b) Input membership functions for IMEP. (c) Output membership functions for output gains.

ΔReplacement Set-Point		Integrated Error				
		-2	-1	0	1	2
Error	-2	+2	+2	+2	+1	0
	-1	+2	+2	+1	0	-1
	0	+2	+1	0	-1	-2
	1	+1	0	-1	-2	-2
	2	0	-1	-2	-2	-2

(a)

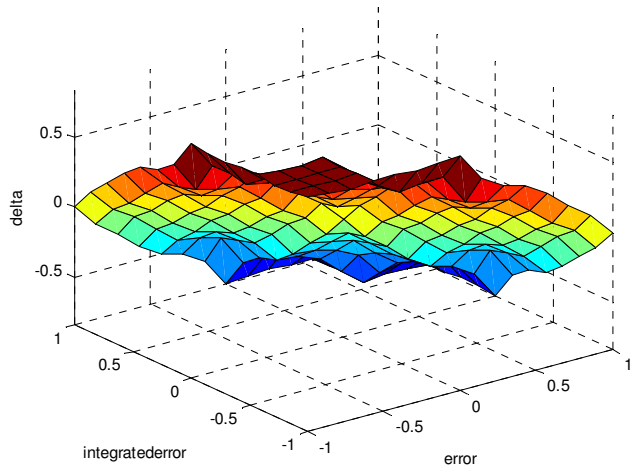

(b)

ΔReplacement Set-Point Gain		IMEP				
		0	1/4	2/4	3/4	1
Speed	0	0	0	0	0	0
	1/4	0	1/4	3/4	2/4	1/4
	2/4	0	2/4	1	3/4	1/4
	3/4	0	2/4	1	3/4	1/4
	1	0	2/4	3/4	2/4	1/4

(c)

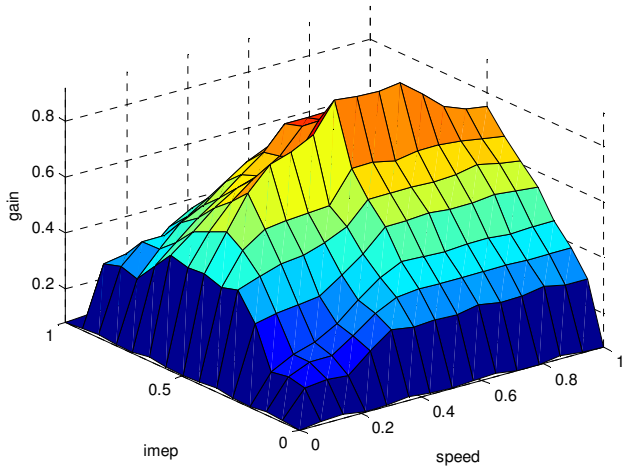

(d)

Figure 6: Rule-base for Δ replacement set-point (a) and its control surface (b). Rule-base for Δ replacement set-point gain (c) and its control surface (d).

$\Delta 1^{st}$ Pulse Timing Set-Point		Integrated Error				
		-2	-1	0	1	2
Error	-2	+2	+2	+2	+1	0
	-1	+2	+2	+1	0	-1
	0	+2	+1	0	-1	-2
	1	+1	0	-1	-2	-2
	2	0	-1	-2	-2	-2

(a)

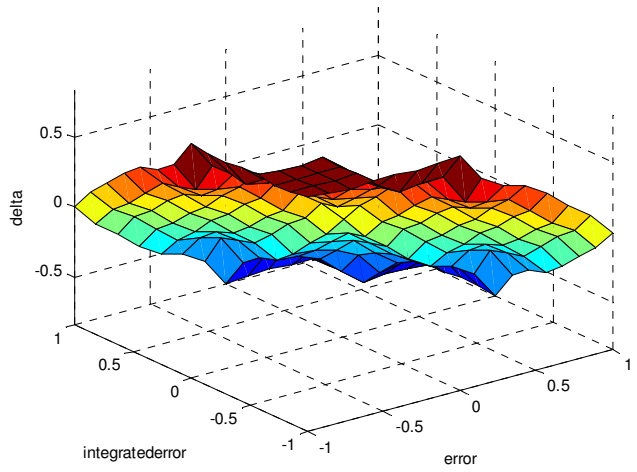

(b)

$\Delta 1^{st}$ Pulse Timing Set-Point Gain		IMEP				
		0	1/4	2/4	3/4	1
Speed	0	0	0	0	0	0
	1/4	0	1/4	3/4	1	1
	2/4	0	2/4	3/4	1	1
	3/4	0	2/4	3/4	1	1
	1	0	2/4	1	1	1

(c)

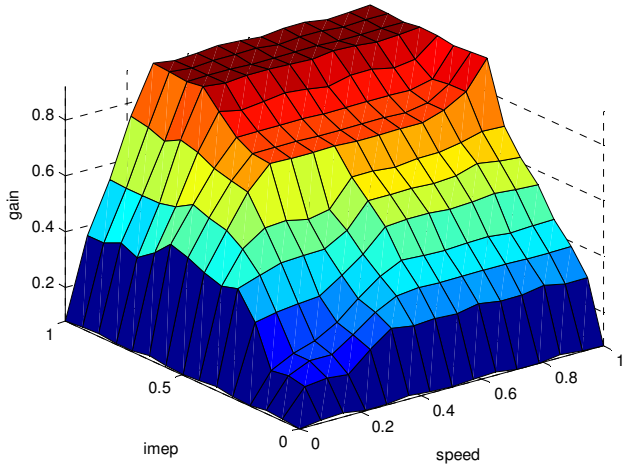

(d)

Figure 7: Rule-base for Δ 1st pulse timing set-point (a) and its control surface (b). Rule-base for Δ 1st pulse timing set-point gain (c) and its control surface (d).

ΔFuel Split Set-Point		Integrated Error				
		-2	-1	0	1	2
Error	-2	-2	-2	-2	-1	0
	-1	-2	-2	-1	0	+1
	0	-2	-1	0	+1	+2
	1	-1	0	+1	+2	+2
	2	0	+1	+2	+2	+2

(a)

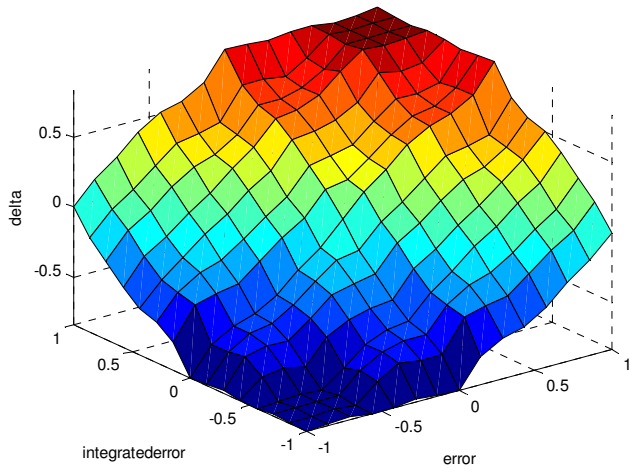

(b)

ΔFuel Split Set-Point Gain		IMEP				
		0	1/4	2/4	3/4	1
Speed	0	0	0	0	0	0
	1/4	0	3/4	3/4	2/4	1/4
	2/4	0	3/4	1	1/4	1/4
	3/4	0	3/4	3/4	2/4	1/4
	1	0	3/4	2/4	2/4	1/4

(c)

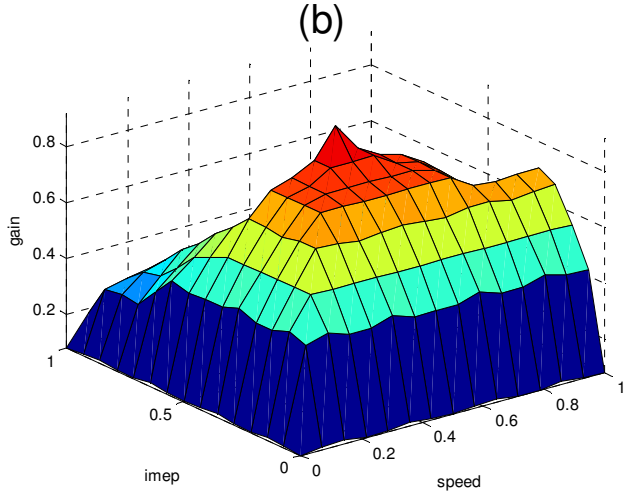

(d)

Figure 8: Rule-base for Δ fuel split set-point (a) and its control surface (b). Rule-base for Δ fuel split set-point gain (c) and its control surface (d).

ΔRail Pressure Set-Point		Integrated Error				
		-2	-1	0	1	2
Error	-2	-2	-2	-2	-1	0
	-1	-2	-2	-1	0	+1
	0	-2	-1	0	+1	+2
	1	-1	0	+1	+2	+2
	2	0	+1	+2	+2	+2

(a)

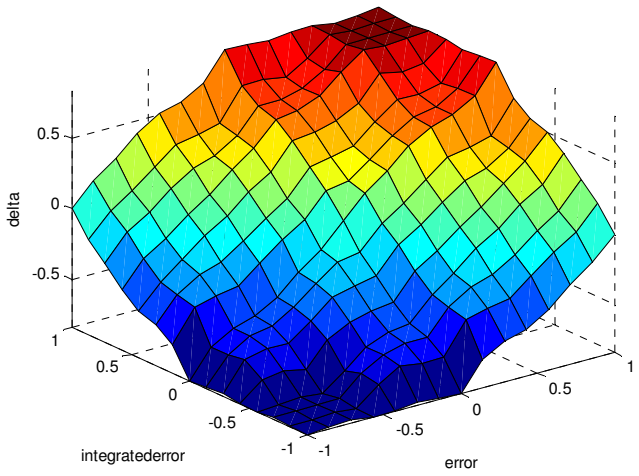

(b)

ΔRail Pressure Set-Point Gain		IMEP				
		0	1/4	2/4	3/4	1
Speed	0	0	0	0	0	0
	1/4	0	0	1/4	3/4	1
	2/4	0	0	2/4	3/4	1
	3/4	0	0	2/4	3/4	1
	1	0	0	2/4	3/4	1

(c)

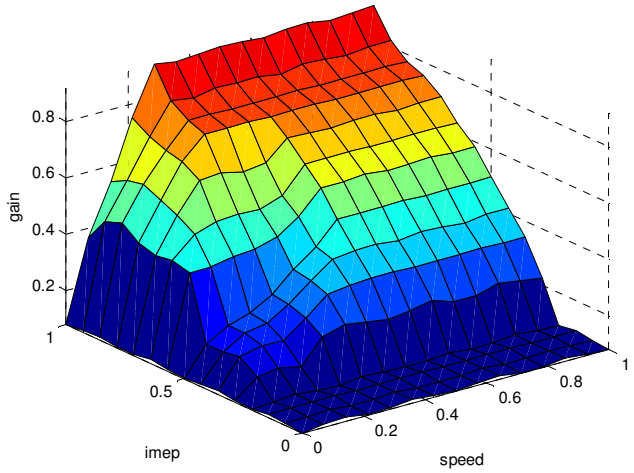

(d)

Figure 9: Rule-base for Δ rail pressure set-point (a) and its control surface (b). Rule-base for Δ rail pressure set-point gain (c) and its control surface (d).

EXPERIMENTAL RESULTS

We implemented the designed control system with our DDF engine test-bed. The engine dynamometer was programmed to run NEDC test. We only show the results of the fourth urban cycle and the sub-urban cycle. There are three cases: no control, use only fuzzy controller, and use both fuzzy controller and fuzzy decision maker.

Figure 10 shows the knock intensity results of all three cases. The knock intensity threshold was set to 0.001 for all engine conditions. It can be seen that the use of both fuzzy controller and fuzzy decision maker delivers the best result in regulating the knock intensity. This is because, with fuzzy decision maker, the adjustment of all parameters can be done appropriately, according to current operating point.

Figure 11 contains the replacement ratio of all three cases. Since the control system enables the engine to operate nearer to optimum points, CNG is used more during most operating points.

Figure 12 shows the first pulse timing of all three cases. We can see a more advanced timing when the fuzzy system is used to reduce knock.

Figure 13 contains fuel split of all three cases. Fuel split decreases to reduce knock. However, the differences are not so obvious due to the fact that the gain b_3 is set to a low positive number.

Figure 14 shows rail pressure of all three cases. Decreasing rail pressure reduces knock.

Figure 15(a) to (d) in the left column show the fixed output gains h_1 to h_4, respectively for the case when only the fuzzy controller was used while all the output gains h_1 to h_4 adapted according to the rules in the fuzzy decision maker. Figure 15(a) to (d) in the right column show Δ replacement set-point, Δ 1st pulse timing set-point, Δ fuel split set-point, and Δ rail pressure set-point.

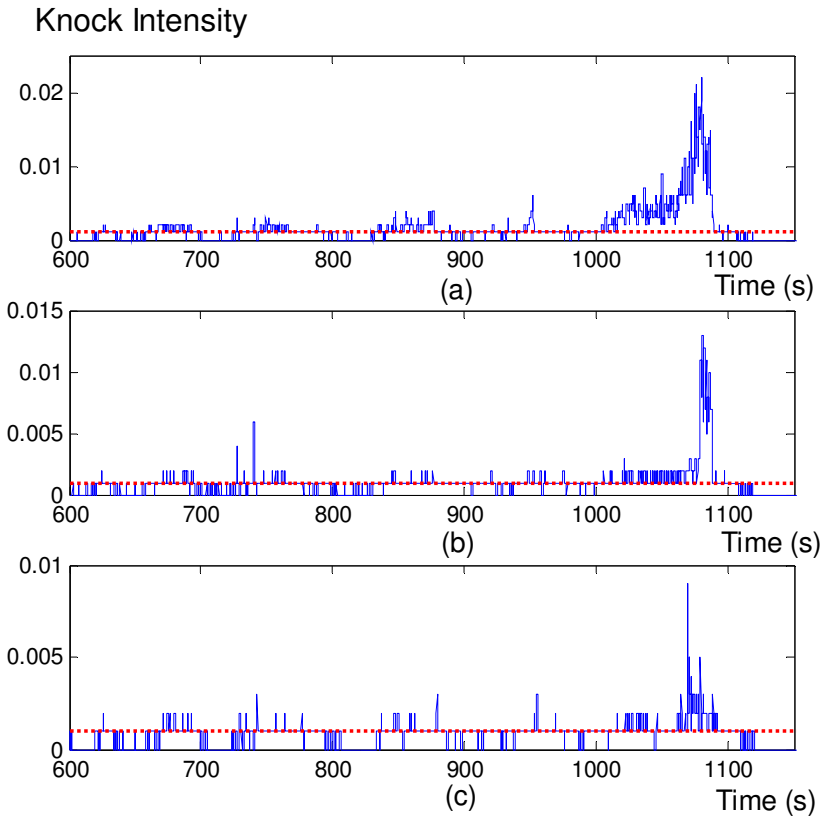

Figure 10: Knock threshold values (red, dash line) and Knock intensity (blue, solid line) for three cases. (a) No control. (b) Use only fuzzy controller. (c) Use fuzzy controller and fuzzy decision maker.

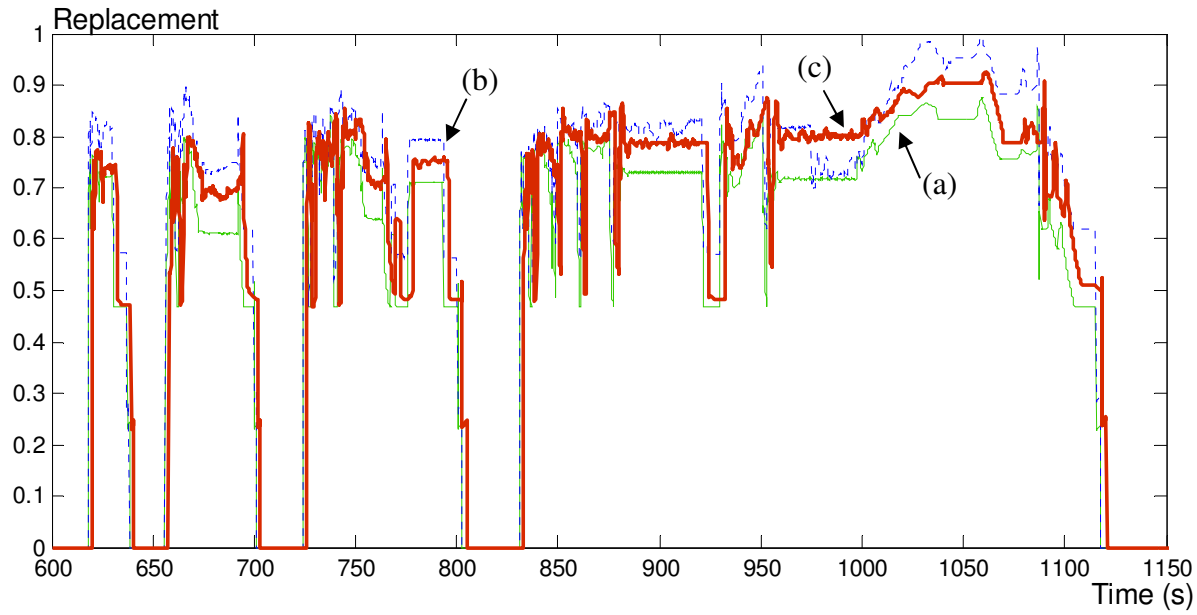

Figure 11: Replacement ratio for three cases. (a) No control (green). (b) Use only fuzzy controller (blue). (c) Use fuzzy controller and fuzzy decision maker (red).

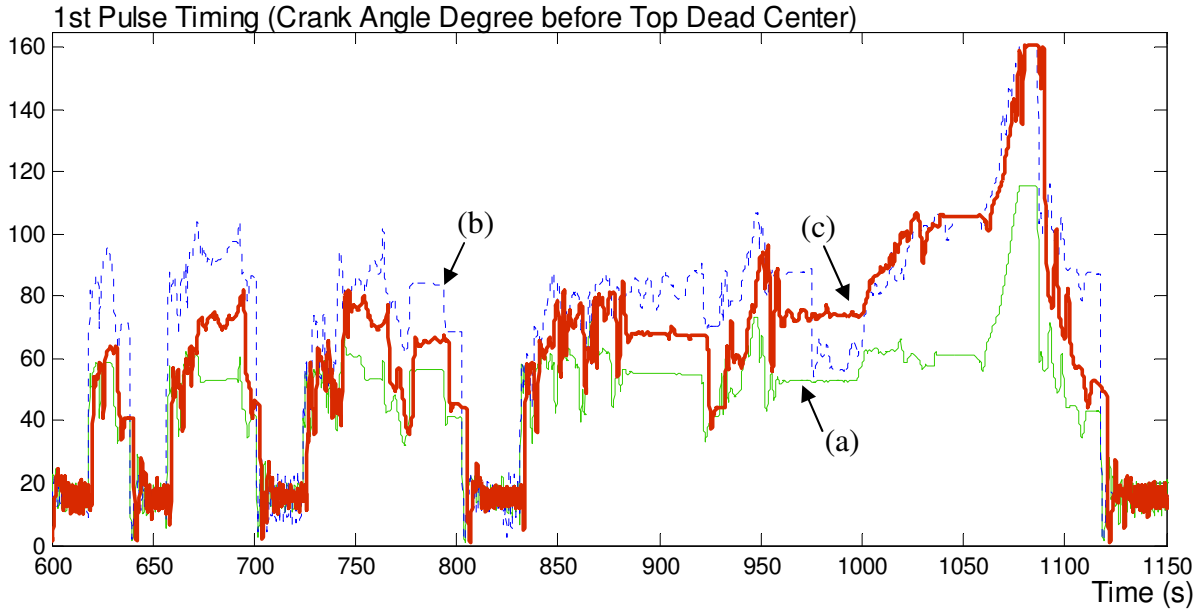

Figure 12: First pulse timing for three cases. (a) No control (green). (b) Use only fuzzy controller (blue). (c) Use fuzzy controller and fuzzy decision maker (red).

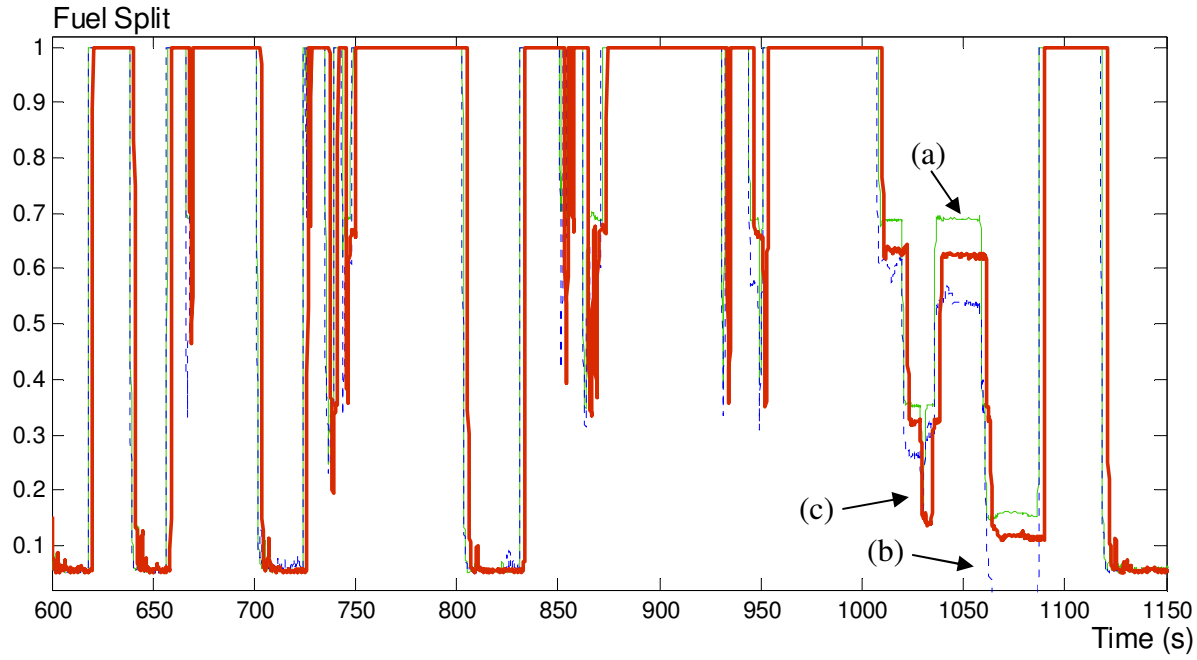

Figure 13: Fuel split for three cases. (a) No control (green). (b) Use only fuzzy controller (blue). (c) Use fuzzy controller and fuzzy decision maker (red).

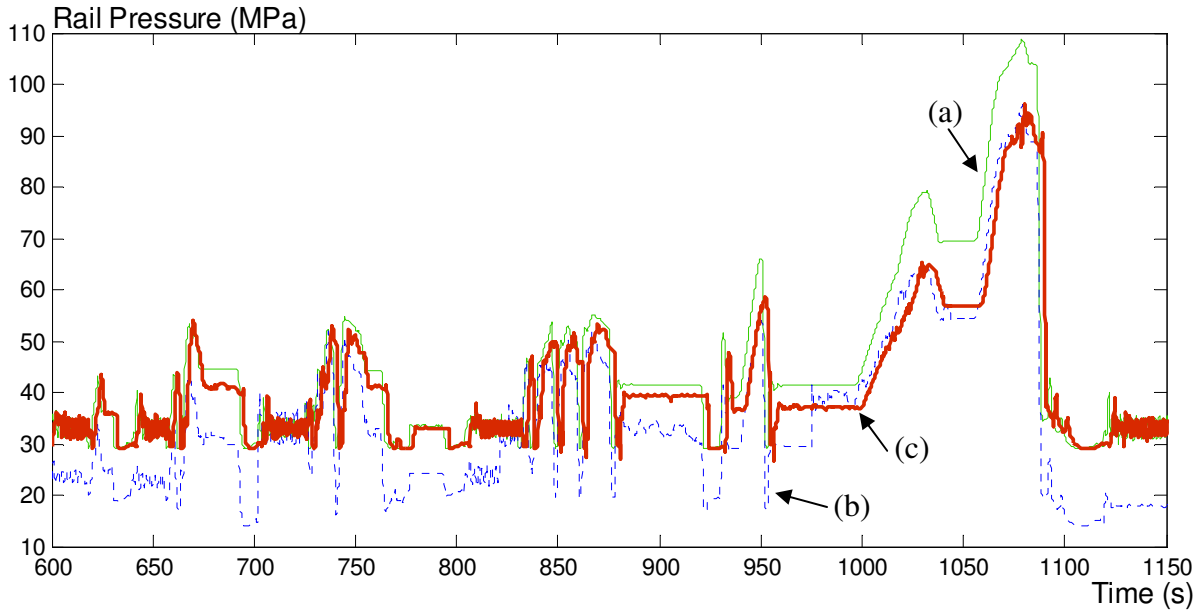

Figure 14: Rail pressure for three cases. (a) No control (green). (b) Use only fuzzy controller (blue). (c) Use fuzzy controller and fuzzy decision maker (red).

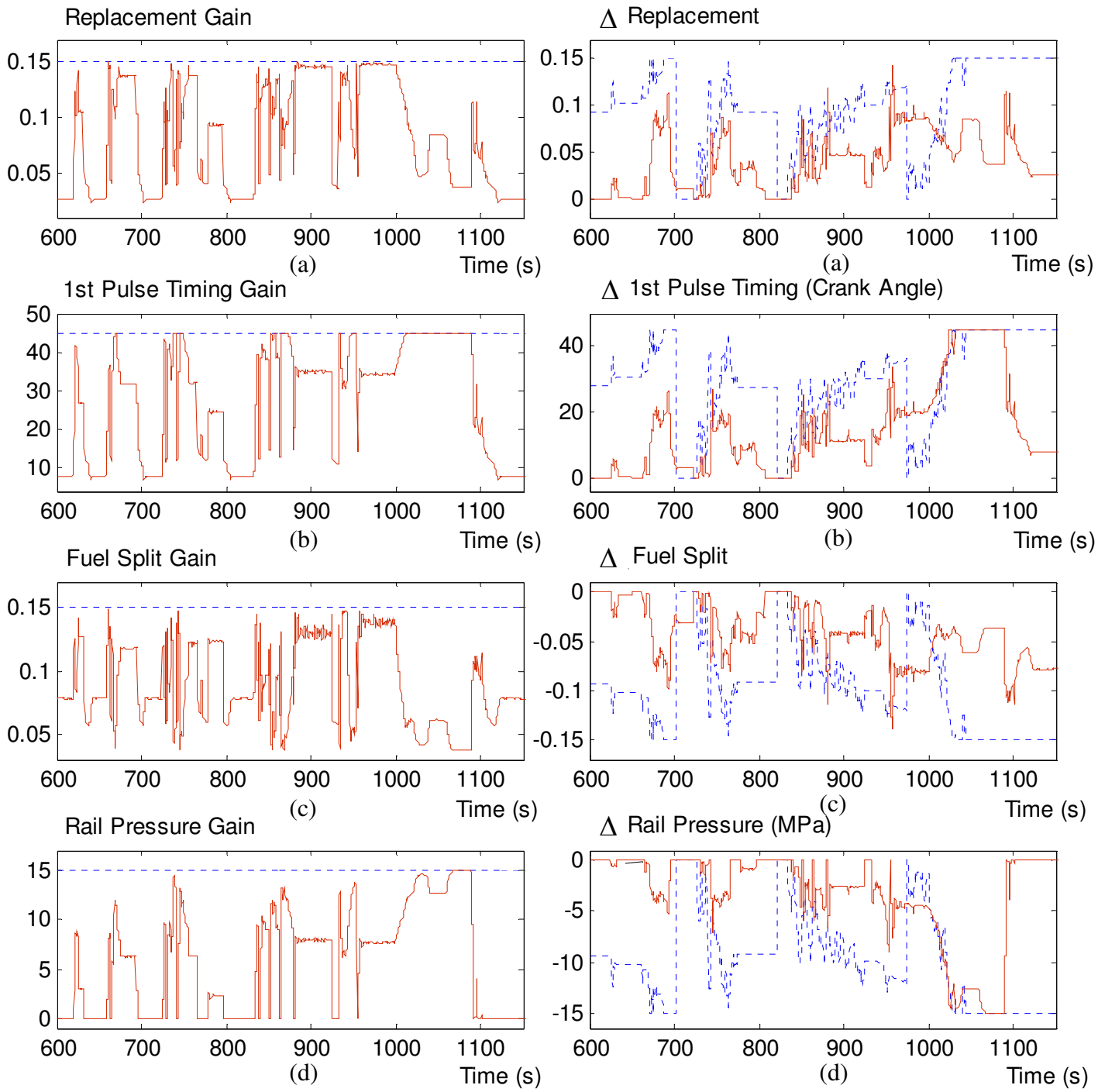

Figure 15: Fuzzy controller output gains (left column) and set-point variation (right column) when only fuzzy controller is used (blue, dash line) and when both fuzzy controller and fuzzy decision maker are used (red, solid line). (a) Replacement. (b) First pulse timing. (c) Fuel split. (d) Rail pressure.

CONCLUSIONS

The engine was commanded to follow the NEDC. The recursive trigonometric interpolation method was used to identify knock intensity. Without knock controller, the maximum knock intensity, from following the NEDC, was 0.02 at frequencies around 60,000-70,000 rad/s. Our proposed knock control system, based on fuzzy logic, regulated the knock intensity at a threshold of 0.001 by using regulated error and its integral as the control system inputs. Replacement ratio by CNG, diesel injection timing, common-rail pressure, and fuel split between the first and second diesel injections were adjusted by the control system. The proposed knock control system has shown excellent result in regulating knock at appropriate intensity values. The use of both fuzzy controller and fuzzy decision maker enhanced knock regulation performance to be better than when only fuzzy controller was used.

Engineers are able to put in their experience in controlling engine to the fuzzy rule-base to effectively regulate knock. In addition to smoother engine operations due to knock avoidance, the engine is able to operate nearer to the optimum points, resulting in more CNG use. The success comes from the facts that

- Control logic comes from human expert experience
- Multiple parameters can be controlled at the same time
- The amount of each actuator action can be adjusted according to current engine speed and load and can be prioritized according to engine sensitivities to various actuator strategies

There are still more work left for future researches. They are listed as follows.

- Each cylinder can be treated separately
  In this paper, we treated each cylinder equally and applied equal amount of actuation to each cylinder. However, knock varies by cylinder-to-cylinder basis. Therefore, it should be beneficial to treat each cylinder separately.
- Locations of knock sensors
  The locations of knock sensors are very important to knock identification. In this paper, we put a knock sensor near cylinder#2, which is where we have an in-cylinder pressure sensor installed. However, one could attempt to find a more suitable knock sensor location.
- Threshold selection
  Because threshold is what we want our knock intensity to follow, threshold selection is very important and often is the most difficult task to find appropriate ones. More effort may be spent on finding optimal threshold that delivers good performance, good efficiency, and low emissions.
- On-line emission test
  Emissions such as CO, NOx, particulate, and HC may be measured. Their effects should be put in the rule-base to choose the right amount of actuation.
- Knock prediction using fuzzy logic
  Fuzzy logic can be used to identify knock from several sensors in order to prevent knock from happening.
- Fuzzy learning control
  Using the learning ability of the fuzzy system, learning fuzzy system can be used to learn to effectively regulate knock at different operating points.
- Actual implementation on a commercial truck

Fuzzy control usually consumes computational resources, especially fuzzy learning control. Attempt should be made to apply these control systems to real world commercial trucks whose ECUs usually contain microcontrollers with limited resources.

REFERENCES

[1] Kiencke, U. and Nielsen, L., Automotive Control Systems: For Engine, Driveline, and Vehicle, Springer, NY, 2005.

[2] Zhu, G. G., Haskara, I, and Winkleman, J., "Closed-Loop Ignition Timing Control for SI Engines Using Ionization Current Feedback," *IEEE Transactions on Control Systems Technology* **15**:416-427, 2007.

[3] Giorgetti, N., Ripaccioli, G., Bemporad, A., Kolmanovsky, I. V., Hrovat, D., "Hybrid Model Predictive Control of Direct Injection Stratified Charge Engines," *IEEE/ASME Transactions on Mechatronics* **11**(5):499-506, 2006.

[4] Yue, S. and Li, P., "Automatic Knock Control System," presented at the 5th World Congress on Intelligent Control and Automation, Hangzhou, China, 2004.

[5] Bolander, W. J. and Milunas, R. S., "Knock Control Using Fuzzy Logic," U.S. Patent 5 560 337, October 1, 1996.

[6] Ettefagh, M. M., Sadeghi, M. H., Rezaee, M., Khoshbakhti, R., and Akbarpour, R., "Application of a New Parametric Model-Based Filter to Knock Intensity Measurement," *Measurement* **43**:353-362, 2010.

[7] Hou, J., Qiao, X., Wang, Z., Liu, W., Huang, Z., "Characterization of Knocking Combustion in HCCI DME Engine Using Wavelet Packet Transform," *Applied Energy* **87**:1239-1246, 2010.

[8] Zhang, Z., Saiki, N., Toda, H., Imamura, T., and Miyake, T., "Detection of Knocking by Wavelet Transform Using Ion Current," presented at the 2009 Fourth International Conference on Innovative Computing, Information and Control, 2009.

[9] Fiolka, J., "A Fast Method for Knock Detection Using Wavelet Transform," presented at the 2006 MIXDES, Gdynia, Poland, 2006.

[10] Thomas, J. H., Dubuisson, B., and Dillies-Peltier, M. A., "Engine Knock Detection from Vibration Signals Using Pattern Recognition," *Meccanica* **32**:431-439, 1997.

[11] Vulli, S., Dunne, J. F., Potenza, R., Richardson, D., and King, P., "Time-Frequency Analysis of Single-Point Engine-Block Vibration Measurements for Multiple Excitation-Event Identification," *Journal of Sound and Vibration* **321**:1129-1143, 2009.

[12] Boland, M. D. and Zoubir, A. M., "Identification of Time-Varying Non-Linear Systems with Application to Knock Detection in Combustion Engines," presented at the 1997 IEEE TENCON.

[13] Stotsky, A. A., Automotive Engines: Control, Estimation, Statistical Detection, Springer, Berlin, 2009.

[14] Wannatong, K., Akarapanyavit, N., Siengsanorh, S., and Chanchaona, S., "Combustion and Knock Characteristics of Natural Gas Diesel Dual Fuel Engine," SAE paper number 2007-01-2047.

[15] Nwafor, O. M. I., "Knock Characteristics of Dual-Fuel Combustion in Diesel Engines Using Natural Gas as Primary Fuel," *Sadhana* **27**:375-382, 2002.

[16] Thayaparan, C., Monohar, Muthuraman, S., "Study of Combustion Phenomena in Diesel Engine for Proper Development of Power with Less Knocking," *Journal of Engineering and Applied Sciences* **2**:435-439, 2007.

[17] Grondin, O., Chauvin, J., Guillemin, F., Nguyen, E., and Corde, G., "Combustion Parameters Estimation and Control Using Vibration Signal: Application to the Diesel HCCI Engine," presented at the 47th IEEE Conference on Decision and Control, Cancun, Mexico, December 9-11, 2008.

[18] Hillion, M., Chauvin, J., and Petit, N., "Controlling the Start of Combustion on an HCCI Diesel Engine," presented at the 2008 American Control Conference, Washington, USA, June 11-13, 2008.

[19] Shahbakhti, M. and Koch, C. R. , "Control Oriented Modeling of Combustion Phasing for an HCCI Engine," presented at the 2007 American Control Conference, New York, USA, July 11-13, 2007.

[20] Bengtsson, J., Gafvert, M., Strandh, P., "Modeling of HCCI Engine Combustion for Control Analysis," presented at the 43rd IEEE Conference on Decision and Control, Paradise Island, Bahamas, December 14-17, 2004.

[21] Saikaly, K., Rousseau, S., Rahmouni, C., Le Corre, O., and Truffet, L., "Safe Operating Conditions Determination for Stationary SI Gas Engines," *Fuel Processing Technology* **89**:1169-1179, 2008.

[22] Shaomei, F., Zhentao, L., and Zhaoda, Y., "Knock Prediction for Dual Fuel Engines by Using a Simplified Combustion Model," *Journal of Zheijiang University Schence* **4**(5):591-594, 2003.

[23] Passino, K. M. and Yurkovich, S., Fuzzy Control, Addison Wesley, USA, 1998.

CONTACT INFORMATION

Contact Withit Chatlatanagulchai at mailing address:

Department of Mechanical Engineering
Faculty of Engineering
Kasetsart University
50 Phaholyothin Road,
Bangkok 10900, Thailand

or email address: fengwtc@ku.ac.th

ACKNOWLEDGMENTS

We would like to thank Ittidej Moonmangmee for knock literature survey.